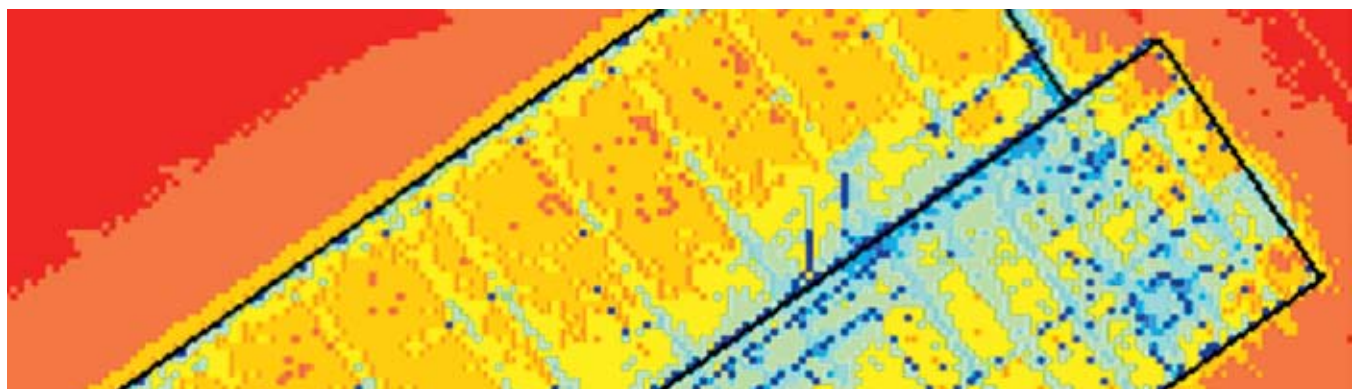


# GNSS Indoors Fighting the Fading

## Part 3

PROF.-DR. GÜNTER HEIN, ANDREAS TEUBER, UNIVERSITY FAF MUNICH



GNSS

Tracking low-power spread spectrum GNSS signals inside buildings is complicated by the effects of various architectures and building materials on signals passing through them. In this final installment of a three-part series, the authors identify and measure some of the key variables affecting the actual Galileo signal-in-space indoors and outline a model for their behavior.

In the first part of this series, we extracted some key parameters that characterize the properties of signal propagation under given geometric conditions between transmitter and receiver.

These parameters are arrival rates and amplitudes of individual signals and so-called clusters that are manifestations of the fading phenomena. In order to determine and to quantify these parameters, we deployed a dedicated hardware set-up and applied statistical methods of analysis.

The second part of the series focused on building materials and their dielectric properties. Numerical simulations as well as various test setups enabled us to compute these properties deterministically. Both the analysis of signal transmission and structural factors can be translated into modeling approaches — with a channel model and a transmission model, respectively, as the outcomes.

This third and final part of the series will now describe how the actual Galileo signal-in-space behaves in a particular building to determine whether we can confirm some of the predictions of the aforementioned models.

### Galileo Measurements

In this part, we would like to turn to a future scenario: a real Galileo signal that is about to penetrate a building. Readers of the first part of this series may remember the residential-like building located at the town of Berchtesgaden that was used as one of the test buildings for the channel sounder measurements. This structure is also used for our measurements of the Galileo signals.

Although the building is located within the Galileo Test Environment (GATE), which is equipped with Galileo transmitters on the surrounding mountains, for our test a helicopter was deployed in order to cover elevations and azimuths as flexibly as possible.

The receiving equipment consisted of two functionalities: First, the capability to measure the voltage so as to directly infer the attenuation effects of the building materials; second, the capability to record the received signal spectra, which provides insights into how the original signal is distorted. Details on the configuration and the hardware that we employed are given later in the description of the airborne and the indoor test configurations.

### Observation Sites

Without doubt, it is meaningful to start the investigations by determining relationships among the various locations of transmitter and receiver. Thus, 15 helicopter positions at six different azimuths and three different elevations were selected.

Figure 1 shows a footprint of the helicopter's transmit positions. The building in which the receiving equipment was located is depicted as yellow rectangle



FIGURE 1 Nominal footprint of helicopter-borne Galileo signal transmitter positions

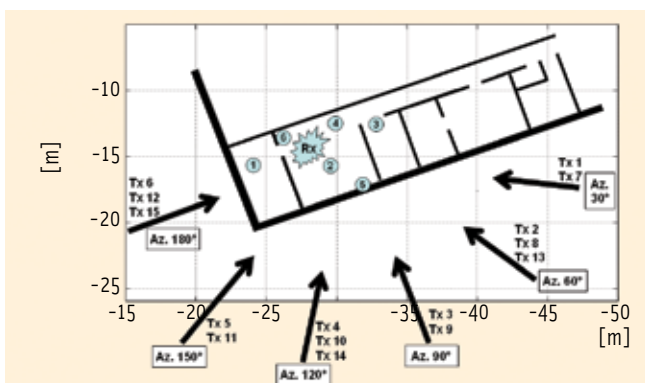


FIGURE 2 Receiver (Rx) position distribution inside test building and azimuths to some of the transmitters (Tx)

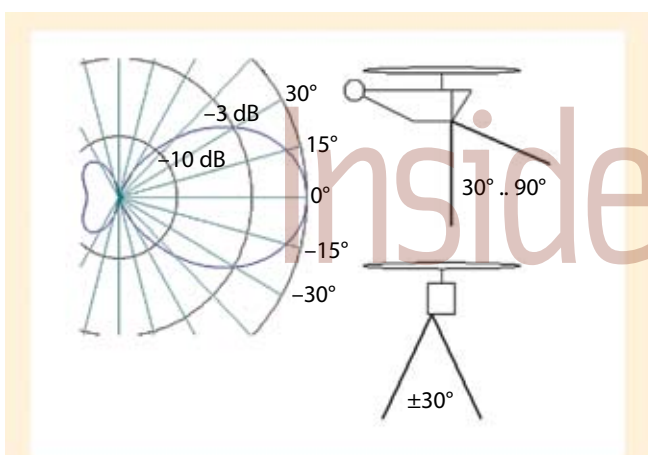


FIGURE 3 Tx antenna pattern and illumination from the mount at the helicopter

in the left part of the figure. In fact, we varied the distances between helicopter and building in order to maintain a constant flight altitude, which was sufficiently high for the flight permission, but still convenient to the pilot for visual naviga-

tion. In order to be able to compare the signal voltages, these had to be normalized to a helicopter distance of 1,000 meters using the free space loss conditions.

Furthermore, the receiver antenna was moved among six different points inside the building, as seen in **Figure 2**. For simplification, in the following discussion transmitter positions will be referred to as Tx positions and receiver positions as Rx positions.

The field campaign took place over two days, with two hours of airborne operation each day. In order not to disturb the reception of the GPS L1 C/A-code signals necessary for navigating the helicopter to the nominal transmitting locations, we decided to transmit on the E6 signal. Some reference measurements confirmed that the principal results can also be applied to Galileo L1.

## Airborne Setup

The E6 band (center 1278.75 MHz) is mainly used by military radar and amateur radio. We did the signal synthesis according to the Galileo Signal in Space Interface Control Document (SIS-ICD). The code generators and the BOC modulation were already implemented. The only simplification was to omit the data generator because data content has no effect on the power level and the spectral properties of the signal.

The signal generation was done using two baseband signals and an I/Q modulator; the digital part of the baseband processor was implemented in a field programmable gate array (FPGA). Our test design required a maximum output power of 27 dBm (0.5 W); so, a power amplifier had to be added to the standard configuration.

To be independent from the power net of the helicopter, we added a LiPo (lithium polymer) rechargeable battery and a stabilizing DC/DC-converter. The design allows four hours of stable operation. The transmitter was installed in the helicopter with a helical antenna mounted on the skid of the aircraft. During the measurements, the transmitter was controlled by a notebook computer using the Ethernet connection.

The antenna had a gain of 7 dBi and a radiation pattern as portrayed in the left panel of **Figure 3**, which also reveals the dependency of the field strength on the aspect angle of the point of observation. Because of the almost symmetrical construction of the antenna, it was sufficient to use this same pattern for all observation planes as long the helical axis was defined as reference.

The left-hand diagram in Figure 3 is normalized to the maximum field strength (=1 or 0 dB). Under the assumption of a spatial bandwidth of -3 dB, the characteristics of the antenna result in a 60-degree radiation lobe. The middle and right-hand diagrams in Figure 3 illustrate the illuminated ranges after fixing the antenna at the helicopter.

## Indoor Equipment Configuration

We deployed two different receiving antennas: an omnidirectional antenna to receive all multipath signals at the same time and an experimental helical antenna. The radiation pat-

tern of the latter shows -3 dB angles of only  $\pm 18.5$  degrees, leading to a high gain of 14 dBi. This antenna was used to discover the directions of the multipath signal. A special fixture allowed us to change the azimuth and elevation of the main receive direction.

Before accessing spectra and voltage information, the received Galileo signal had to be down-converted to an intermediate frequency (IF). After passing the IF filter and a gain controllable amplifier, the conditioned signal was available for monitoring.

The output signal of the converter was distributed to the detector and the spectrum analyzer. We measured the DC output voltage of the detector using a digital voltmeter. The spectrum analyzer and voltmeter were connected to a PC using IEEE 488 interfaces. A block diagram of the down-converting and monitoring scheme is given in **Figure 4**.

## Transforming Voltages into Signal Levels

The output of the digital voltmeter indicating the received signal power level was recorded every second during the first day's helicopter flight and every 100 milliseconds during the second day's flight. A moving average of 20 samples was calculated throughout the flights on both days for filtering purposes.

We then converted the filtered voltages into signal power levels by connecting a calibrated signal generator tuned to the E6 frequency to the receiver instead of the antennas. Using this setup, we obtained the relationship between level and detector voltage presented in **Figure 5**.

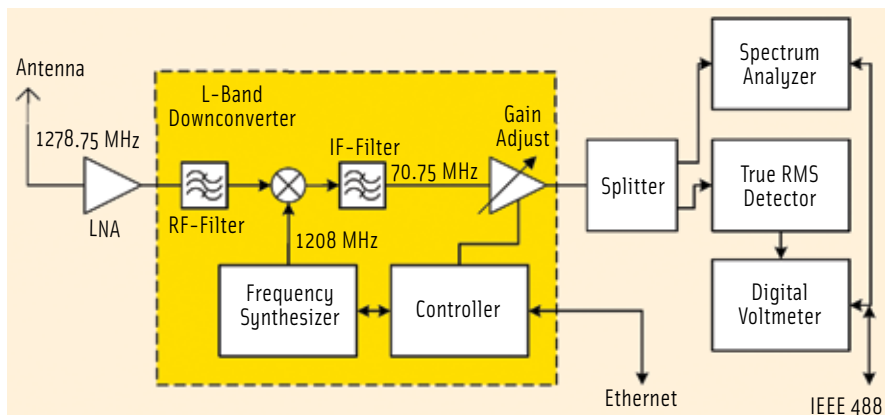


**FIGURE 4** Receiver with signal level detector and spectrum analyzer

As illustrated by the graph of our measurements, the resulting curve is quite linear from -85 to -60 dBm. However, it flattens out between -110 and -100 dBm.

This is not due to the detector but rather to the thermal noise generated by the receiver (mainly by the LNA) itself. The setup allows accurate measurements down to -100 dBm at a bandwidth of 80 MHz.

To simplify the data processing we evaluated a polynomial approximation of the curve, which is also shown in **Figure 5**. Using this function we calculated the levels for all measurements out of the filtered voltages.

In a final step we selected the values for all measurements using the timing

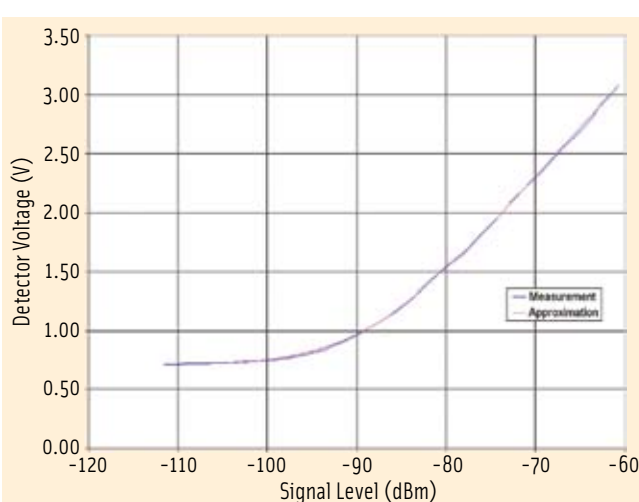


**FIGURE 5** Relationship between level and detector output voltage

records. **Table 1** shows a sample of the pre-processed data.

### Pre-Processing the Signal Spectra.

One sample of the spectrum analyzer consisted of 601 data value pairs (frequency bins with a width of 86.25 kHz each, power in dBm). To evaluate the absolute spectral density (dBm/Hz) at the antenna output, we needed to adjust

Time	Freq.	Site in Building	Heli Site	RX Azimuth [°]	RX Elevation [°]	Voltage [V]	Filtered Voltage [V]	Level [dBm]
20070614114712	E6	1	2	0	30	1.050	1.05050	-88.0264798
20070614114724	E6	1	2	60	30	1.590	1.55300	-79.9949416
20070614114734	E6	1	2	120	30	0.940	0.93600	-90.9907857
20070614114746	E6	1	2	180	30	1.030	0.98350	-89.6551749
20070614114757	E6	1	2	240	30	0.830	0.82600	-95.1520963
20070614114813	E6	1	2	300	30	0.950	0.99450	-89.3697928
20070614114931	E6	1	2	0	60	0.970	1.00100	-89.2048083
20070614114923	E6	1	2	60	60	0.840	0.90650	-91.9252603
20070614114914	E6	1	2	120	60	0.880	0.91350	-91.6947963

**TABLE 1.** Sample of the pre-processed voltage data



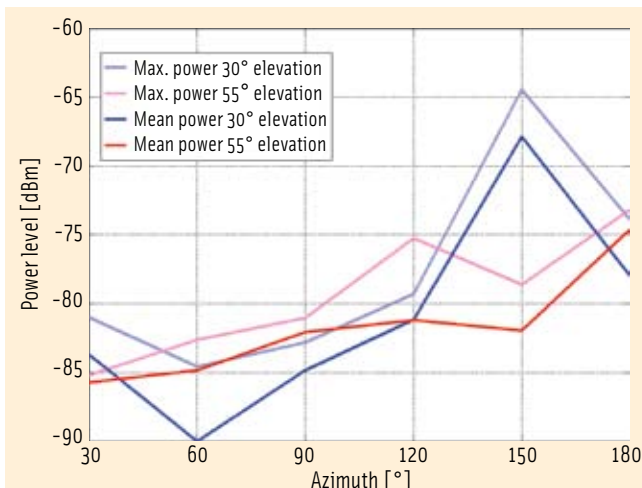


FIGURE 6 Power level of Rx1 with respect to azimuth (x-axis) and elevation (colors)

Reference to...	Parameter	# of configurations
... location of Tx antenna	Azimuth	6
	Elevation	3
... location of Rx antenna	Size of the room	3
	Distance to (exterior) wall/roof	varying
	Number of walls	3
... properties of the building	Wall/ceiling materials	n/a
	Path length through wall/ceiling	varying
... adjustment of Rx antenna	Azimuth	6
	Elevation	2

TABLE 2. Parameters that likely affect signal power level

the readout with a correction factor that took care of the resolution bandwidth of the analyzer and the conversion gain of the receiver setup. Because both factors were fixed, we were able to compare different spectra.

## Correlating Azimuth Elevation and Signal Power

We started using the omnidirectional antenna to investigate signal power levels, generating power profiles in relationship to azimuth and elevation. As an example, **Figure 6** shows the received normalized power level recorded at Rx 1 for six azimuths and elevations of 30 degrees (blue) and 55 degrees (red). The bold lines represent the mean signal power extracted from recording windows of about 45 seconds.

Due to unanticipated movements of the helicopter and the maneuvers needed to maintain the current posi-

only wall is very short, which also results in a rather high power level.

Although for the azimuths of 90 and 120 degrees (Tx 3 and Tx 4, respectively) only one (exterior) wall lies between transmitter and receiver, the distance between receiving antenna and exterior wall is larger. At the azimuth of 60 degrees the conditions are worst, since the signal has to pass through one exterior and one interior wall under an unfavourable angle. For the azimuth of 30 degrees the conditions are slightly better, perhaps due to the vicinity of a doorway (see Figure 2) that replaces the interior wall.

For the 55-degree elevation, the signal power profile is flatter. On the one hand, this is due to the fact that a signal is probably not received directly via the window. On the other hand, for four of the six azimuths (Tx 7 to Tx 10) the signal is expected to enter the room via

tions, we faced a latent risk of straying outside the lobe of maximum gain of the direction-sensitive transmitting antenna. Thus, the collected mean signal power could be significantly below the maximum signal power. In order to check this, Figure 6 contains the maximum signal power as well (in light blue and pink color, respectively).

Clearly, the maximum power level for the 30-degree elevation (blue lines) is at an azimuth of 150 degrees. This can easily be explained by the vicinity of an external window in the room where Rx 1 was located. Furthermore, at an azimuth of 180 degrees the distance to the

the ceiling. The distance to the ceiling is equal for all points; so, the red curve looks very smooth for these points.

Nevertheless, a small but steady increase occurs from 30 to 120 degrees azimuth. The reason for this could be the longer signal path between the uttermost part of the building (roofing tiles) and the receiving antenna because the building has a pitched roof.

Clearly, for the signals with lower azimuth the angle between the longitudinal axis of the building and the propagation path is more acute. Consequently, the entry point at the roof is higher, and the propagation path in the attic room between the roofing tiles and the ceiling is longer. The strong increase of the power level at 180 degrees can be explained by the perpendicular crossing of the wall.

In general, therefore, we can state that the received power level depends on azimuth and elevation. This is in accordance with what has emerged from the channel model described previously. However, because the power level diagrams cannot exclusively be explained by azimuth and elevation dependency, other factors are significantly influencing the results.

## Proposed Modelling Effort

Let us take an extended view on the possible influencing factors. **Table 2** distinguishes between the location of the Tx antenna, the location of the Rx antenna, the direction-sensitive characteristics of the Rx antenna, and the properties of the building.

Due to the limited time and location of our field tests, however, we could only consider a limited number of configurations, as reflected in the third column of Table 2. For example, information about the wall materials was too sparse to provide a sufficient variety of cases.

Intrinsically, the diversity of parameters would call for an integrated approach of processing, e.g., a multiple regression. Unfortunately, not every data set yields information about each of the parameters. Thus, we needed to pursue a sequential approach to data analysis.

## The Wall-Distance Rule

For example, let's consider the relationship of signal power levels to the location of the Rx antenna combined with the distance of the closest wall. A basic requirement for this investigation is that the signal propagates through one wall only and enters the building via the exterior wall or the window.

**Figure 7** shows 17 individual cases (12 from Rx 1, 4 from Rx 2, and 1 from Rx 3). These cases are distinguished by whether, as a result of Tx/Rx geometry, a high probability exists of partial signal propagation through a window (red color) or a definite signal propagation only through the wall (blue color).

The red and blue asterisks denote the collected individual values, and the like-colored lines shows the corresponding linear regression functions. The following formulas for the linear regression have been derived.

$$P_{\text{wall}} = -68.0 - 3.3d \quad (1)$$

$$P_{\text{wind}} = -60.6 - 2.4d$$

with  $P$  denoting the signal power level and  $d$  denoting the distance from the wall or window, respectively.

From Equation 1, we can infer that each meter of displacement from the wall leads to a decrease in terms of signal power: about 3.3 dB for the wall case and about 2.4 dB for the window case. The difference between the two cases at a very (theoretically) close distance to wall/window is hardly more than 7 dB. In fact, this value coincides with the related attenuation factors between concrete and glass that were shown in the second part of this series dealing with the transmission model.

## Some Initial Conclusions

After analyzing all the parameters under investigation, we can draw the following conclusions regarding the signal power level of a Galileo signal propagating in an indoor environment:

- The signal power level decreases with increasing distance from the furthestmost point at which the signal propagation path enters the building.
- As long as there is only one layer of building material to be penetrated

(e.g., only a window or a wall), the attenuation gradient only depends on the distance to this uttermost point and is independent of the actual location of the receiver indoors. A first coarse assessment indicates that the signal power decreases by about 3 dB

per meter of distance from the exterior wall.

- If two layers of material must be penetrated (e.g., roof and ceiling with an attic room between) the relationship will be more complicated and the gradient will be significantly larger (probably up to 10 dB or more per meter of distance).
- The signal power level decreases with increasing elevation of the signal source. This is inverse to the outdoor situation where tropospheric effects attenuate low-elevation signals.
- With respect to the azimuth, the signal power level is maximal at a direction perpendicular to the closest exterior wall of the building.
- Corners of a building seem to be more favorable entry points than plane walls.

## Discovering Multipath Directions

We continued our work using the helical beam antenna in order to investigate whether we could detect significant incident directions caused by reflections of the signals. Because our tests required two different Rx antenna adjustments in elevation and six different adjustments in azimuth, time constraints limited the measurements to only two Rx locations and eight Tx locations.

**Figure 8** presents the results for Tx 12 and Rx 2 at a 30-degree elevation, a case in which we might detect the effects of multipath.

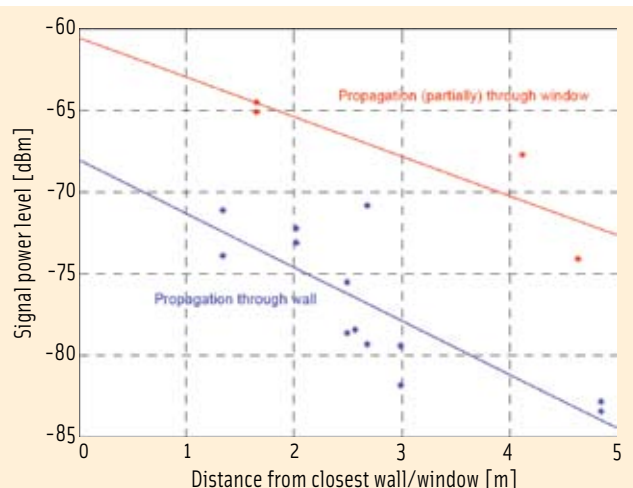


FIGURE 7 Signal power levels in relation to distance from wall/window

The signals from the opposite direction from the transmitter (0° azimuth) and from azimuth 120° are stronger than from the actual direction of the Tx location (180° azimuth). This probably occurs because two walls lie in the direct path between Tx and Rx while, due to the geometry inside the building, the signal might well enter the building through a window, propagate through the doorway, and reach the antenna via a reflection at the northern interior wall (0° azimuth) of the room in which the receiver (Rx 2) is located.

Alternately, the signal may enter the room after undergoing diffraction at another window and reach the antenna under the 120° azimuth.

## Profiling the Signal Spectra

To make the spectra measurements, we

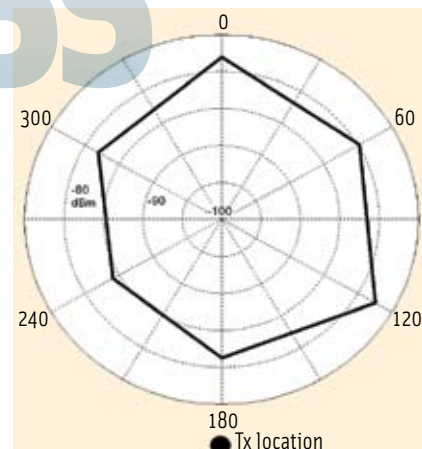


FIGURE 8 Azimuth-dependent power levels of Tx12 measured at Rx 2

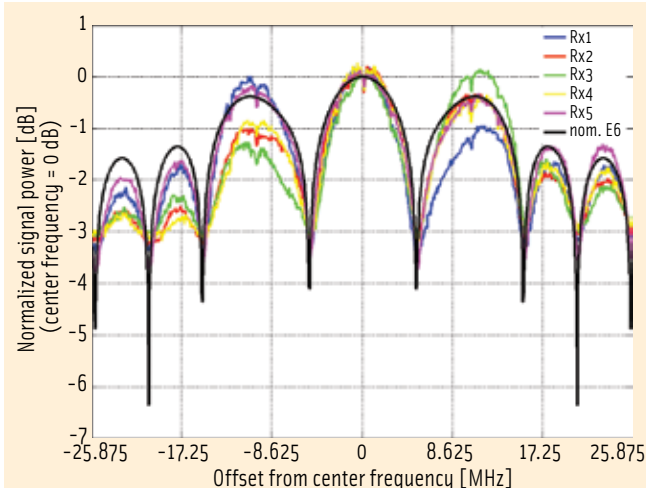


FIGURE 9 Normalized measured spectra from Tx 10 at five receivers and the nominal spectrum (black)

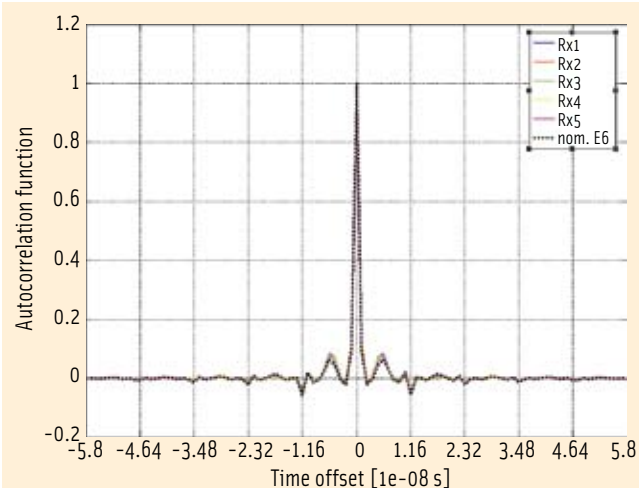


FIGURE 10 Autocorrelation functions compared to nominal one (black)

occupied six Rx locations and eight Tx locations. This resulted in a total of 44 utilizable spectra. Spectra of four of the Tx-Rx combinations did not pass the quality check. Due to time constraints those records could not be repeated. For this part of the test, the omnidirectional Rx antenna was deployed.

We divided analysis of the resulting data into two parts. First, we investigated the shapes of the measured spectra and compared these to the shape of an ideal nominal signal. Second, we transformed the signal spectra into the time domain in order to investigate the shape of the autocorrelation function.

In order to directly compare the measured spectra with the nominal one, the raw signal power data had to be processed in two further stages:

- Each spectrum was normalized to the power level at the center frequency. We averaged the nine most central frequency bins (bandwidth 776 kHz) to determine this power level.
- The variance of each spectrum was normalized to one.

**Figure 9** provides the results for one of the eight transmit locations (Tx 10). The different colors represent the receiver locations. The bold black curve demonstrates the shape of the nominal E6 signal.

After analyzing all Tx locations, we can make the following observations:

- The main lobe of the measured spectra is not always the lobe that contains the most energy. In 25 cases of

the 44 measured spectra (57 percent), the center lobe captured the most energy. In 12 cases (27 percent) the first lobe on the right side captured the most energy and in the remaining 7 cases (16 percent), the first side-lobe on the left did so.

- Whereas the lobes of the nominal signal have edgeless maxima and sharp minima, the maxima of the measured spectra are sharper in most of the cases and the gaps between the maxima are wider. Thus, the energy is distributed less effectively over the bandwidth.
- We suspect that the maxima of the side lobes of the measured spectra are farther from the main lobe than is the case for the nominal spectrum. In fact, the frequency distance between the main and the right side-lobe is 369 kHz larger than nominal. Keeping in mind that the first side-lobe of the composite E6 signal appears about 10 MHz apart from the main lobe, the detected shift spreads the lobe distance by about 3.5 percent.

## Autocorrelation Function

We have limited our attention thus far to the signal in the frequency domain. However, we can change the signal into the time domain by applying the inverse fast Fourier transformation (IFFT).

**Figure 10** shows the results of this transformation in terms of the autocorrelation function for one of the eight

transmit positions (Tx 10). We sampled 600 points in the frequency domain 86.25 kHz apart from each other. This resulted in a distance of 1.16 microseconds between two sampling points in the time domain.

We needed to find metrics that would allow us to quantify the distortions of the autocorrelation function. We selected the following three criteria as sufficient illustration of the distorting effects. We will refer to these dimensionless variables as *quality criteria*.

- *Quality criterion 1:* The higher the maximum amplitude of the first side peak relative to the main peak, the larger the signal distortion.
- *Quality criterion 2:* The larger the cumulative area covered by the autocorrelation function, the larger the signal distortion.
- *Quality criterion 3:* The larger the residuals of the function from the nominal signal — expressed by the standard deviation — the larger the signal distortion.

A visual inspection of the spectra showed that each of the three criteria serves as a suitable indicator in the majority of the cases. This can be confirmed numerically by computing the correlation coefficients between the vectors that contain the criteria for all 44 Tx-Rx-combinations.

In fact, only the combination of all three criteria is capable of forming a powerful and universal quality param-



eter, because in some of the 44 cases one of the three criteria features a significant deviation from the others.

After a normalization of the three criteria with respect to amplitude and variance we are allowed to execute arithmetic operations on them. We decided to compute the mean and named the result the joint *quality parameter*. Note the inverse relationship in these results: due to the definition of the three criteria, a decrease in the quality parameter corresponds with an increase in the signal quality.

## Establishing Model Parameters

Our desire to discover the influencing variables that affect the behavior of the quality parameter of the autocorrelation function leads us back to the candidate parameters in Table 2 and the initial conclusions we drew when considering the signal power levels. Unfortunately, a first glance at the spectral data shows that some of these candidates cannot be adopted. Exemplarily, Table 3 shows the three quality criteria with respect to the three Tx antenna elevations do not exceed their standard deviation, which proves that this variable will not provide a suitable metric.

Furthermore, in the matter of signal power levels we detected the following phenomena: a low incident angle with the exterior wall together with a short distance from this wall provides higher power and, further, corners are preferred entry points. In principle, this relationship is still valid for the spectral data. However, it seems that more than one property has to be present to make a significant difference.

A look at Figure 11 might explain this. Due to the longer distance to the closest exterior wall, Rx 2 should be spectrally unfavorable compared to Rx 1. However, this single fact alone is not yet enough to make it a significant influence variable affecting the quality parameter.

If we consider the signal propagation path from Tx 1, the situation of Rx 2 is also unfavorable due to the larger angle of incidence. Consequently, the combination of these two factors probably

leads to a significant influence on the quality parameter of the spectra that neither of them demonstrates alone.

Finally, Rx 2 also suffers from the larger distance of the propagation path from a corner of the building. The combination of the three factors makes them definitely influence the quality parameter.

An exhausting analysis of the available data gave us some insight into the effects of the interrelated geometry of the building's and the Rx-Tx directions as shown in Figure 11. Our next task was to express measurable quantities that sufficiently represent the geometrical effects. We refer to them as *influencing variables* (denoted here in bold letters), and we can characterize them with the following statements:

- (1) *The shorter the distance from the corner of the building the better the signal quality.*
- (2) *The shorter the distance from the entry point the better the signal quality.*
- (3) *The larger the intersecting angle between the signal and the exterior wall the better the signal quality.*
- (4) *The smaller the intersecting angle between the vector going through the Tx antenna and the Rx and the vector going through the nearest corner of the building and the Rx antenna the better the signal quality.*
- (5) *The larger the number of windows or the bigger the area that the windows cover from the viewpoint of the Rx antenna the better the signal quality.*
- (6) *The smaller the number of walls that the geometrically direct signal path has to penetrate the better the signal quality.*

## Fuzzy Logic: Verifying the Variables

As already illustrated earlier by means of Figure 11 we cannot draw simple deterministic relationships about the spectral qualities of the received signal indoors as we did for the signal power levels. This means that one isolated statement is not capable of predicting the signal quality

	Quality criterion 1	Quality criterion 2	Quality criterion 3
Tx elevation 30°	0.10	0.34	0.012
Tx elevation 55°	0.09	0.33	0.010
Tx elevation 80°	0.10	0.32	0.010
$\sigma$ of complete sample	0.01	0.03	0.003

TABLE 3. Results for quality criteria for different Tx elevations

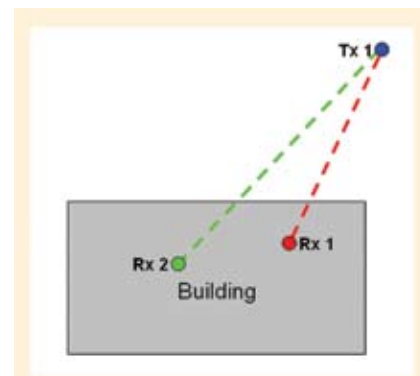


FIGURE 11 Schematic visualization of different propagation paths

inside a building very well. In contrast to this, applying combinations of the six mentioned statements can frequently provide a good prediction of the signal quality.

Hence, we know that the modelling of the signal distortions on the basis of geometrical information is a rather complicated and not easily applicable task. Nevertheless, we wanted to find out if this modelling is possible in principle. Initially, we were interested in finding a mathematical tool that could assist us.

Artificial neural networks (ANN) and fuzzy logic appeared to us as promising approaches. Because the amount of data available to us could not serve as a sufficient training sample for an ANN, we decided to apply fuzzy logic. This approach allows us to adopt rather directly the statements about influencing variables presented earlier, while the terms *bigger* and *better* have to be transformed into quantized steps (e.g. into stages such as *big*, *medium*, *small* or *very good*, *good*, *satisfactory*, *moderate*, *weak*)

These adopted statements are then called rules. A little more than 20 rules have been formulated, most of them combining more than one statement in order to achieve the required significant rela-

	Model fit quotient
Rx 1	0.27
Rx 2	0.23
Rx 3	0.17
Rx 4	0.13
Rx 5	0.32
Rx 6	0.61

TABLE 4. Results for model fit quotient for different Rx locations

tions with respect to the signal quality.

Using the example of Figure 11 the following rule would be appropriate:

If  
the distance from the entry point is short

and  
the intersecting angle between the signal and the exterior wall is large

and  
the intersecting angle between the vector going through the Tx antenna and the Rx and the vector going through the nearest corner of the building and the Rx antenna is small

then

the signal quality is very good.

After some iterative steps with respect to rule formulation, the outcomes of the fuzzy modelling approach were finally compared to the actually computed signal quality parameters introduced earlier. We are able to compare these after normalizing the model output to determine whether both parameters have the same variance and the same mean.

For the comparison we computed the residuals and determined the standard deviation. Because we perpetually deal with dimensionless variables, the standard deviation does not become meaningful until relating it to the mean.

Fortunately, due to the definition of the three quality criteria, our parameters are always positive real numbers. Therefore, we can state that the smaller the quotient of the standard deviation divided by the mean is, the better the modelling approach fits.

**Table 4** refers to this quotient as a model fit quotient. In fact, this value is rather small for the Rx positions 1 to 4, still moderate for Rx 5, but significantly higher for Rx 6 (where the standard deviation is more than half of the mean).

Thus, we can conclude that — apart from some deviations at the receiver position Rx 6 — we are able to model the quality parameter by means of appropriate geometric influencing variables.

## What the Galileo Measurements Yielded

In fact, we have been able to determine suitable parameters that have an influence on the signal power level indoors as well as on the magnitude of distortion of the Galileo signal. For the signal power level we were able to find simple relationships between one parameter and the signal power as a target value.

In assessing signal distortion, however, a single parameter often does not determine the result. Frequently, the interaction of different parameters creates a significant effect on the quality parameter. The fuzzy logic approach provides a suitable tool to express these interactions as rules and, hence, sufficiently describes the actual signal quality in most of the cases using only the six previously defined input parameters.

## Conclusion

This three-part column intended to give an overview of the investigation on the properties of GNSS signals propagating indoors. These properties embraced among others the relative geometry of transmitter and receiver as well as the building materials. Finally, after presenting the gathered insights from the developed channel and transmission models in the first two parts, we investigated the received signal power level and the received shapes of the spectra of the true Galileo signal in space.

An analysis based on measurements from 8 to 15 transmitter positions and 3 to 6 receiver positions delivered suitable parameters with which to describe Galileo signal fading satisfactorily. Interestingly, some of the parameters affecting the power level seem to differ from those causing the distortion of the signals.

We attempted to show how suitable information can be obtained from observations collected using dedicated setups. Moreover, it even paved the way to the point of model generation. However, this

only provides a suitable description of the phenomena caused by indoor signal propagation.

As for the near future, these models can be useful for simulation purposes. It remains to be determined whether we will ever be able to master the difficult step of implementing the models into a GNSS receiver's signal-processing chain. We can be sure that a lot more time and effort will be needed before the performance of indoor GNSS will be comparable to its performance outdoors.

## Manufacturers

The Galileo signal generator developed and constructed by **Work Microwave GmbH**, Holzkirchen, Germany, was a prototype derived from the one designed in the INDOOR project funded by the German Aerospace Center (DLR). The helical transmitting antenna mounted used on the helicopter — loaned for the tests by **IfEN GmbH**, Poing, Germany — had been designed within the GATE (Galileo Test and Development Environment) project. The spectrum analyzer used in the indoor environment was an Agilent 8563EC from **Agilent Technologies**, Santa Clara, California, USA. The deployed receiving antennas were an omnidirectional GPS 704 X pinwheel antenna from **NovAtel, Inc.**, Calgary, Alberta, Canada, which was used to receive all multipath signals at the same time, and an experimental helical beam antenna designed and constructed in the laboratory of Work Microwave GmbH.

## Acknowledgement

We would like to thank the German Aerospace Center (DLR) for the funding of the project FKZ 50 NA 0510. Furthermore, we would like to thank Dr. Günter Prokoph and Sebastian Ebenbeck of Work Microwave GmbH for their essential contributions during the Galileo signal field campaign. In particular, we would like to dedicate this work to Sebastian Ebenbeck who tragically died in a recent car accident.

## Authors

"Working Papers" explore the technical and scientific themes that underpin GNSS programs and






applications. This regular column is coordinated by **PROF. DR.-ING. GÜNTER HEIN**. Prof. Hein is a member of the European Commission's Galileo Signal Task Force and organizer of the annual Munich Satellite Navigation Summit. He has been a full professor and director of the Institute of Geodesy and Navigation at the University of the Federal Armed Forces Munich (University FAF Munich) since 1983. In 2002, he received the United States Institute of Navigation Johannes Kepler Award for sustained and significant contributions to the development of satellite naviga-

tion. Hein received his Dipl.-Ing and Dr.-Ing. degrees in geodesy from the University of Darmstadt, Germany. Contact Prof. Hein at <Gunter.Hein@unibw-muenchen.de>.



**Andreas Teuber** is research associate at the Institute of Geodesy and Navigation at the University FAF Munich. He received his diploma in geomatics engineering from the University of Hannover, Germany. Currently, his main subjects of interest are indoor positioning in general and applying WLAN technology for positioning purposes in particular. 

# InsideGNSS